

# MpoxVLM: A Vision-Language Model for Diagnosing Skin Lesions from Mpox Virus Infection

**Xu Cao\***

*University of Illinois Urbana-Champaign, USA*

XUCAO2@ILLINOIS.EDU

**Wenqian Ye\***

*University of Virginia, USA*

WENQIAN@VIRGINIA.EDU

**Kenny Moise**

*Université Quisqueya, Haiti*

KENNY.MOISE@UNIQ.EDU

**Megan Coffee†**

*NYU Grossman School of Medicine, USA*

MEGAN.COFFEE@NYULANGONE.ORG

## Abstract

In the aftermath of the COVID-19 pandemic and amid accelerating climate change, emerging infectious diseases, particularly those arising from zoonotic spillover, remain a global threat. Mpox (caused by the monkeypox virus) is a notable example of a zoonotic infection that often goes undiagnosed, especially as its rash progresses through stages, complicating detection across diverse populations with different presentations. In August 2024, the WHO Director-General declared the mpox outbreak a public health emergency of international concern for a second time. Despite the deployment of deep learning techniques for detecting diseases from skin lesion images, a robust and publicly accessible foundation model for mpox diagnosis is still lacking due to the unavailability of open-source mpox skin lesion images, multimodal clinical data, and specialized training pipelines. To address this gap, we propose MpoxVLM, a vision-language model (VLM) designed to detect mpox by analyzing both skin lesion images and patient clinical information. MpoxVLM integrates the CLIP visual encoder, an enhanced Vision Transformer (ViT) classifier for skin lesions, and LLaMA-2-7B models, pre-trained and fine-tuned on visual instruction-following question-answer pairs from our newly released mpox skin lesion dataset. Our work achieves 90.38% accuracy for mpox detection, offering a promising pathway to improve early diagnostic accuracy in combating mpox.

**Keywords:** Vision-language models, Mpox, Infectious diseases, Skin Lesions

**Data and Code Availability** We are using our own mpox dataset that we have built and collected, currently the largest of its kind globally, to conduct experiments for both baseline models and our proposed model. The dataset will be made available to other researchers upon submission of a formal request in accordance with IRB guidelines. To facilitate access, we will use a dedicated website to streamline the dataset sharing process. Additionally, the code used in our experiments will be released [here](#)

**Content Warning:** This paper contains medical images that some may find sensitive.

## 1. Introduction

Mpox is a zoonotic disease caused by the orthopoxvirus monkeypox virus (MPXV) (Mitjà et al., 2023a,b; Siegrist and Sassine, 2023; Laurenson-Schafer et al., 2023; Lu et al., 2023) that has affected over 99,518 individuals in an outbreak across 122 countries as of Sep 7, 2024. In the USA, there are 32,063 mpox cases with 58 associated deaths. Its spread across all inhabited continents has demonstrated sustained and prolonged human-to-human transmission, which was not previously recognized before 2022. The World Health Organization (WHO) declared its global spread a Public Health Emergency of International Concern (PHEIC) in 2022. Undetected infections delayed isolation and helped further transmission (Bragazzi et al., 2022). In July 2024, more than 100 laboratory-confirmed cases of clade 1b mpox were reported in

---

\* Equal contribution

† Corresponding Author



Figure 1: Examples of skin lesion images in our datasets. We have 86 classes (including mpox) in total. The medical images have been processed to remove any potential information leakage, such as hospital tags or disease information labels.

South and North Kivu in the DRC and four neighboring countries — Burundi, Kenya, Rwanda, and Uganda— none of which had previously reported endemic mpox cases (Rivers et al., 2024; Sahin et al., 2022). The actual number of cases are expected to be higher, given case positivity and testing rates, as many clinically compatible cases have not been tested. Thus, it is very urgent to develop a computer-aided diagnosis method to detect mpox automatically, with high sensitivity for screening.

Recently, the potential of deep learning, particularly through the use of convolutional neural network (CNN), has been explored to enhance mpox case detection using skin lesion images (Khan et al., 2023; Sizikova et al., 2022; Rampogu, 2023; Chadaga et al., 2023; Harris, 2024; Soe et al., 2024). However, vision models are susceptible to false negatives and errors, as relying on a single skin lesion image for disease detection can be highly inaccurate. In real-world clinical practice, medical professionals assess skin lesion images in conjunction with clinical, point of care and past laboratory values, epidemiological, demographic, and other relevant multimodal data to diagnose mpox. Additionally, many of the vision-

based models developed for skin lesion analysis are trained on small, imbalanced dermatological datasets, often of low quality, including images of monkeys, drawings, and microscopic virus images (Islam et al., 2022).

After the blooming of large language models (LLMs) and vision-language models (VLMs) (Omiye et al., 2024), it becomes a wide trend to develop foundation models for different medical domains (Li et al., 2023b; Huix et al., 2024). Recent studies showed that VLMs finetuned with large-scale, broad-coverage biomedical figure-caption and visual question-answer datasets can effectively learn semantic characteristics via visual instruction tuning (Liu et al., 2024; Li et al., 2024). Thus, connecting visual representations with multimodal text information from biomedical language models becomes increasingly critical to adapting foundation models for medical image classification, particularly in the challenging setting of multimodal data deficiency like mpox (Cheng et al., 2023) and other skin lesion imaging tasks (Zhou and Gao, 2023).

In our study, we develop a VLM-based mpox diagnosis algorithm, MpxVLM, designed specifically for the identification of mpox virus skin lesions in photographic skin lesion images together with easily accessible clinical information. Our algorithm’s evaluation across our newly collected mpox dataset with multimodal information aims to ensure its effectiveness for individuals of different skin types, genders, ages, and lesion sites, thus facilitating timely and accurate diagnosis of mpox infections. The contributions are summarized as follows:

1. We propose the first Vision Language Model (VLM) framework MpxVLM for mpox detection and its training pipeline. This is the first foundation model diagnosing skin lesions from mpox virus infection.
2. We collected a new multimodal mpox diagnosis dataset from publicly available information including skin lesion images and clinical record from 2,914 samples.
3. The experiment results on our newly collected dataset show that the proposed MpxVLM achieves the best performance results than the previous state-of-the-art methods.

## 2. Related Works

**Mpox History and How it spread.** Historically, the mpox was predominantly in children exposed to host animals, in outbreaks in Central and West Africa since the 1970s and later due to imported pets in the Midwestern United States in 2003, but the outbreak in Nigeria in 2017 and the later global outbreak since 2022 has been predominantly in adults (Breman et al., 1980; Zinnah et al., 2024; Luma et al., 2022; Guarner et al., 2022). The role of sexual networks was underappreciated until 2022 when transmission was largely among men who have sex with men (MSM) (Allan-Blitz and Klausner, 2024; Pekar et al., 2024). Given the changing epidemiology and the associated stigma and denial, cases, even in a known outbreak, were often missed; in one study, only 23% of healthcare workers used appropriate personal protective equipment for all encounters with patients later confirmed to have mpox (Marshall et al., 2022). Mpox is often mistaken for another infection, such as sexually transmitted infections and viral exanthems, but also less common autoimmune and infectious causes. The lesions develop from unremarkable pimples over days to weeks into pathognomonic, umbilicated pustular lesions, but are infectious throughout and transmission often occurs before diagnosis is suspected. Associated symptoms (fever, sore throat, lymphadenopathy, and pain) vary between patients and resemble other diseases, so clinical suspicion usually focuses on the rash. Given a missed infection can lead to the further community - or less commonly, healthcare clinic transmission - it is important to have a screening test and clinical support for clinicians with little experience diagnosing mpox. Thus, it is very meaningful to develop and deploy computer-aided diagnosis solutions for those countries influenced by mpox (Bleichrodt et al., 2024).

**Mpox Diagnosis with Deep Learning.** Deep learning has shown promise in classifying skin lesions in dermatology (Barata et al., 2019; Liu et al., 2020; Gröger et al., 2023). For mpox, Convolutional Neural Networks (CNNs) have demonstrated effectiveness in identifying disease through the analysis of skin lesion images (Thieme et al., 2023). Initial studies employed CNN models such as MobileNet (Jaradat et al., 2023; Altun et al., 2023), VGG Net (Ahsan et al., 2022a) that were pre-trained using the ImageNet database, and subsequently fine-tuned with either publicly or privately sourced mpox skin lesion image datasets. Sitaula et al. (Sitaula and Shahi, 2022) further pro-

posed an ensemble learning method to combine Xception and DenseNet to predict mpox. Bala et al. (Bala et al., 2023) amassed a dataset comprising 770 skin lesion images, including 279 mpox cases, and introduced MonkeyNet, a model that leverages the architecture of DenseNet alongside multiple data augmentation techniques. Subsequent research has made the Mpox Skin Lesion Dataset (MSLDv2.0) (Ali et al., 2023) publicly accessible, which includes 284 Mpox image samples. However, these datasets are still too small to train reliable models.

**Vision-Language Models (VLMs).** In computer vision, the exploration of VLMs for handling tasks involving multiple modes of data has developed very fast. This interest has sparked new developments in multi-modal large language models (MLLMs), leading to the creation of new innovative tools like GPT-4V (Wu et al., 2023) and Gemini (Team et al., 2023). A key strategy to embed visual information into language models involves the fine-tuning or instruction tuning of large-scale foundational VLMs, such as Flamingo (Alayrac et al., 2022) and MiniGPT4 (Zhu et al., 2023). This technique has been further refined by recent developments like visual prompt tuning (Jia et al., 2022), LLaVA (Liu et al., 2024; Li et al., 2024), InternVL Chen et al. (2024), LLaMA-Adapter (Zhang et al., 2023), and BLIP-2 (Li et al., 2023a), which employ instruction-following LLMs trained on VQA datasets specifically designed for image instruction tuning. The effectiveness of instruction tuning in improving the performance of VLMs on multi-modal vision-language tasks has been demonstrated, highlighting its potential to significantly advance the field.

## 3. Methodology

**Overall Architecture.** Fig 4 illustrates the main workflow of the proposed MpoxVLM framework. It included two encoders and a LLM decoder. The first encoder is a Contrastive Language-Image Pretraining (CLIP) visual encoder and it is frozen during our model training. The second encoder is a Vision Transformer (ViT) classifier encoder self-supervised learning pretrained with our proposed mpox dataset in using masked autoencoder (He et al., 2022). The LLM decoder used in our framework is LLaMA-2-7B Touvron et al. (2023) with 7 billion parameters. Each encoder is connected with the LLM decoder by a two-layer multilayer perceptron (MLP) module as

the alignment between visual features and language features.

Inspired by LLaVA (Liu et al., 2023) and MiniGPT-4 (Zhu et al., 2023), our framework aims to integrate the visual features of skin lesion images and the clinical records of patients into a unified representation, leveraging the LLM to facilitate the diagnosis of mpox. The input of the task comprises a skin lesion image, denoted as  $X_v$ , alongside context-specific prior knowledge, represented as  $X_c$ .

To train the MPOxVLM, we also design question-answer pair from our proposed dataset,  $(X_q, X_o, Y)$ , to guide the model’s learning. The aim of using question-answer pairs as input and output structures is to streamline the integration of visual and textual data. Here,  $X_q$  poses a critical question based on the evaluation of the skin lesion image: "After reviewing this skin lesion image, do you think the patient has mpox?".  $X_o$  is a group of options denoting mpox or non-mpox. In our original dataset,  $X_o$  can be multiple choices including  $> 30$  common skin diseases. In order to let model only focus on the diagnosis of mpox, we set the number of options to two in the training phase. The task of MPOxVLM and other baseline models is to predict an answer  $\hat{Y}$  from the options, which represents the model’s assessment of whether the patient is likely to have mpox.

The proposed MPOxVLM  $F_\theta$  can be formulated as:

$$\hat{Y} = F_\theta(X_v, X_c, X_q, X_o) \quad (1)$$

In the following subsections, we will introduce the structure of MPOxVLM and our training procedure.

### 3.1. Model Design

**Visual Encoder.** Different to previous VLM solutions in medical imaging such as Med-LLaVA, the MPOxVLM framework incorporates dual encoders to process and analyze input image data effectively. The first encoder  $f_{\text{CLIP}}$  is a visual-language encoder, specifically a frozen pre-trained CLIP visual encoder. Within the MPOxVLM framework, this encoder’s role is to extract general visual features from the input mpox image, enabling a detailed visual-language representation of the skin lesion image. The extracted features are then passed through a trainable projection alignment module (a 2-layer MLP). This alignment module is crucial for mapping the visual tokens into text embedding space of the LLM. The second encoder  $f_v$  in the MPOxVLM system is a visual encoder, built upon a pre-trained vision transformer (ViT) classifier

that is specialized in skin lesion image analysis. This encoder focuses on deriving high-level classification insights from the visual data. The output from this visual encoder, particularly the classification token, is directed through another trainable projection alignment module. The purpose of this alignment module is to project the classification token accurately into the LLM’s text embedding space. These dual encoders are important for translating complex visual features into a format that the LLM can seamlessly process and interpret, enhancing the overall visual understanding capability of the MPOxVLM.

**Visual Instruction Tuning for MPOxVLM.** To finetune the LLM within the MPOxVLM framework, our approach aims to synergistically harness the strengths of the pretrained LLM (LLaMA-2) along with the integrated dual visual encoders. For input skin lesion image  $X_v$ , we use the tokenizer from CLIP visual encoder (ViT-L/14-336) to embed the image into tokens. The visual feature is extracted from CLIP’s visual encoder and then the adapter layer to map image features into the LLM’s word embedding space:

$$Z_{\text{CLIP}} = W_{\text{CLIP}} \cdot f_{\text{CLIP}}(\text{Tokenizer}(X_v)), \quad (2)$$

$$Z_{\text{CLIP}} \in R^{d_h \times k}$$

, where  $f_{\text{CLIP}}$  is the CLIP encoder.  $W_{\text{CLIP}}$  is the weight of the linear projection layer.  $d_h$  is the dimension of the LLM embedding.  $k$  is the number of visual tokens.

In the classification path, the input skin lesion image  $X_v$  is tokenized by the same CLIP’s patch embedding layer and then extracted visual tokens by a pretrained ViT for skin lesion image classification. The classification token of the last layer is then fed to an adapter layer to map the classification features into the LLM’s word embedding space.

$$Z_V = W_V \cdot [f_V(\text{Tokenizer}(X_v))]_{\text{CLS}}, \quad (3)$$

$$Z_V \in R^{d_h \times 1}$$

, where  $f_V$  is the ViT encoder for classification.  $W_V$  is the weight of the linear projection layer.  $d_h$  is the dimension of the LLM embedding. CLS means the classification token from the ViT’s output.

For a sequence of length  $L$ , the autoregressive encoder in the LLM for generation mpox diagnosis answer is as follows:

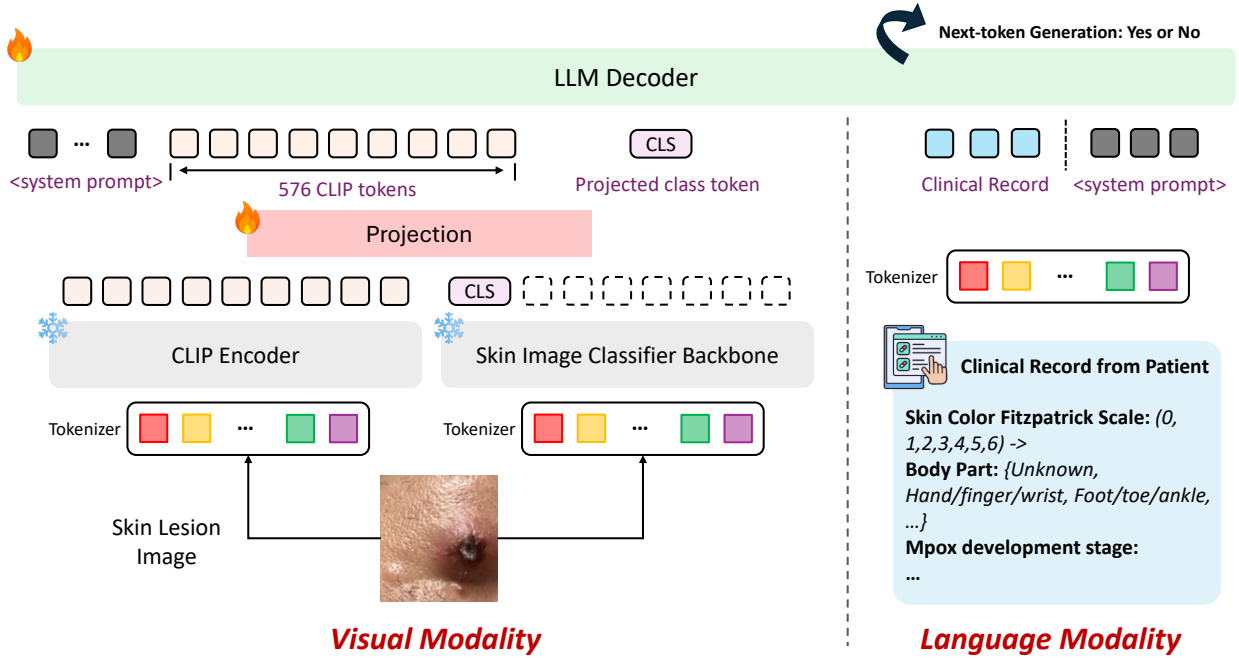


Figure 2: Workflow of the MPOxVLM framework and visual question-answer pair examples.

$$\begin{aligned}
 & p(\hat{Y} | Z_{\text{CLIP}}, Z_V, X_c, X_q) \\
 & = \prod_{i=1}^L p_{\theta}(y_i | (Z_{\text{CLIP}} \oplus Z_V), X_c, X_q, X_o, \hat{Y}_{<i>i}
 \end{aligned}
 \tag{4}$$

, where  $X_q$  is all of the question tokens (the whole question).  $X_o$  is the option tokens.  $\oplus$  is the concatenation operation for latent features.  $\hat{Y}_{<i>i$  is all answer tokens before  $y_i$ .

$$\hat{Y} = f_{\text{LLM}}(Z_{\text{CLIP}}, Z_V, X_c, X_q, X_o)
 \tag{5}$$

, where  $f_{\text{LLM}}$  is the LLM (LLaMA-2-7B).

### 3.2. Training Pipeline

Firstly, we pretrained a ViT encoder (ViT-L-14-336) with the proposed mpox skin lesion dataset. Then, we build the MPOxVLM model with the pretrained ViT encoder as the classification visual encoder and the CLIP encoder (clip-vit-large-patch14) (Radford et al., 2021) as the visual-language encoder. Then, in the following experiment, we freeze the weights of both the CLIP visual encoder and classification visual encoder. The LLM used in our task is LLaMA-2 7B (Touvron et al., 2023). To train the two linear adaptors, we keep

LLM weights frozen and only train alignment layers between the dual visual encoders and the LLM. After pretraining the alignment layers, we keep all weights frozen except the weight of LLMs, and finetune the weight under the mpox visual question answer task.

## 4. Experiments and Results

### 4.1. New Mpox Dataset and Demographic Analysis.

Prior to our work, there are some mpox skin lesion image datasets available (Ahsan et al., 2022b; Jara-dat et al., 2023; Bala et al., 2023; Ali et al., 2023). However, most of the datasets are relatively small and can not be used to train large models. To solve this issue, we proposed a new mpox dataset including both mpox skin lesion image and multimodal clinical information such as patients’ medical history. The comparison of different mpox datasets is presented in Table 1. All of the data in our new dataset is collected and curated by doctors from public sources (medical and news journals, public health websites, and social media). It comprises 1,057 Mpox-positive samples and 1,857 samples of other diseases, totaling 2,914 samples. We have meticulously cropped each image to remove surrounding clothing or backgrounds and to

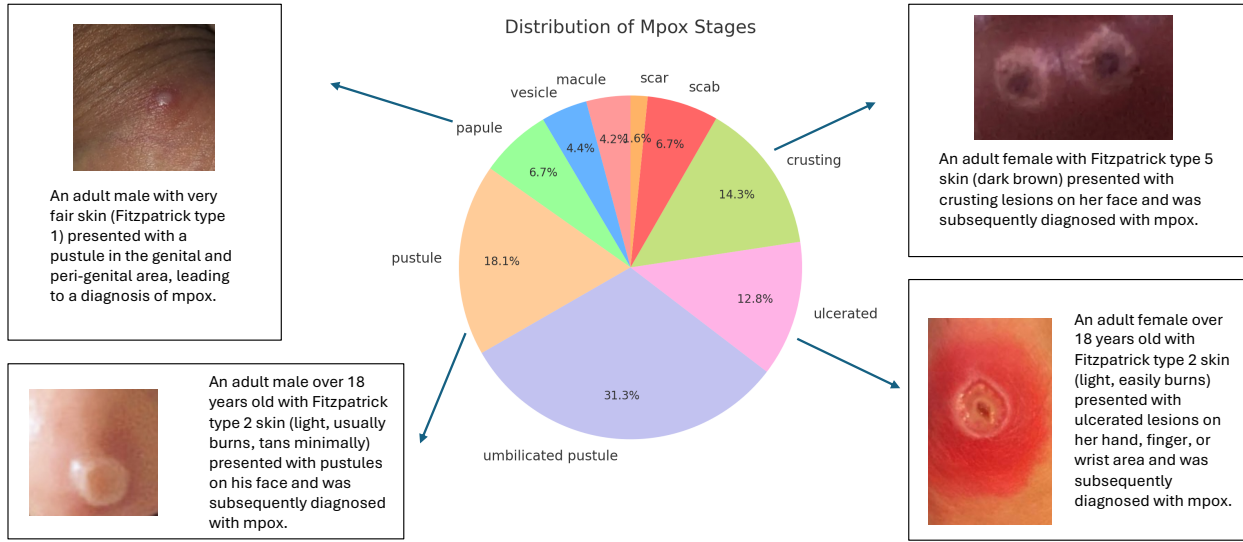


Figure 3: Distribution of Mpx development stages and instruction tuning data in the mpx dataset. The stages of Mpx progression are ordered as follows: macule, vesicle, papule, pustule, umbilicated pustule, ulceration, crusting, scab, and scar.



Figure 4: Mpx skin images in our dataset.

focus on disease lesions and supplemented them with demographic annotations in Figure 3 for skin type (Fitzpatrick scale of 1-6), gender or sex presentation (based on accompanying information or image alone), and age (adult or child). The dataset also included the affected body part and stage of mpx lesions (macule, papule, vesicle, pustule, umbilicated pustule, ulcerating, crusting, scab, to scar) in order to ensure early stages were represented, as many images are of late, classic stages. Doctors carefully selected compara-

tor images from 86 diagnoses that closely resemble mpx. These images were chosen to match key characteristics, including demographic factors (skin type, gender, age), affected body parts (as initial lesions often correspond to the transmission route and area of first exposure), and the epidemiology of diseases commonly mistaken for mpx. Additionally, some diseases that clinicians may be less familiar with were included, recognizing these may be more difficult to distinguish. Infectious disease specialists selected the comparator diseases based on global epidemiology and clinical presentations, using both clinical physician expertise and image searches to find visual mimics. The primary objective of this dataset refinement is to fully leverage the data-centric approach of large foundation models. This approach is aimed at achieving a more accurate representation of data distribution and facilitating a fairer comparison with previously established methodologies.

#### 4.2. Evaluation Metrics.

To evaluate the performance of our model, we use several standard metrics: **Accuracy:** measures the proportion of correctly predicted instances out of all predictions. **Precision:** known as *positive predictive value*. It evaluates the proportion of true positive predictions to the total number of positive predictions. It is useful for understanding the reliability of

Dataset	Mpox Sample Size	All Sample Size	Demographic Information
Ahsan et al. (Ahsan et al., 2022b)*	43	161	✗
Jaradat et al. (Jaradat et al., 2023)*	45	117	✗
MonkeyNet (Bala et al., 2023)	178	492	✗
MSLD v2.0 (Ali et al., 2023)	284	755	✓
Kularathne et al. (Kularathne et al., 2024)	120	120	✗
<b>Ours</b>	<b>1,057</b>	<b>2,914</b>	<b>✓</b>

Table 1: Mpox Dataset Comparison. \* denote original data (without data augmentation). Kularathne et al. (Kularathne et al., 2024) used 120 data to synthesize 1,000 mpox images via DreamBooth (Ruiz et al., 2023).

Methods	Accuracy(%) $\uparrow$	Precision(%) $\uparrow$	Recall(%) $\uparrow$	F1 Score(%) $\uparrow$	AUROC(%) $\uparrow$
Bala et al. (2023)	73.06 $\pm$ 1.79	66.45 $\pm$ 1.37	54.21 $\pm$ 4.21	59.71 $\pm$ 3.63	78.23 $\pm$ 3.04
Thieme et al. (2023)	74.61 $\pm$ 0.78	66.48 $\pm$ 3.33	62.63 $\pm$ 4.21	64.50 $\pm$ 0.89	80.88 $\pm$ 0.61
Sitaula and Shahi (2022)	87.21 $\pm$ 1.74	85.62 $\pm$ 0.08	78.42 $\pm$ 5.79	81.87 $\pm$ 3.24	93.91 $\pm$ 0.66
Ahsan et al. (2022a)	74.42 $\pm$ 1.63	77.36 $\pm$ 1.24	43.16 $\pm$ 4.25	55.41 $\pm$ 3.71	79.55 $\pm$ 2.94
Jaradat et al. (2023)	81.20 $\pm$ 1.41	71.43 $\pm$ 1.56	81.58 $\pm$ 2.11	76.17 $\pm$ 1.81	89.33 $\pm$ 0.80
Altun et al. (2023)	79.46 $\pm$ 0.31	74.14 $\pm$ 1.26	67.89 $\pm$ 1.97	70.88 $\pm$ 0.66	83.38 $\pm$ 0.91
Li et al. (2024)	87.34 $\pm$ 0.55	84.16 $\pm$ 1.89	82.33 $\pm$ 2.51	82.24 $\pm$ 1.22	85.95 $\pm$ 0.73
<b>Ours</b>	<b>90.38<math>\pm</math>0.80</b>	<b>86.77<math>\pm</math>1.85</b>	<b>84.38<math>\pm</math>0.78</b>	<b>85.72<math>\pm</math>1.14</b>	<b>95.16<math>\pm</math>0.72</b>

Table 2: Comparisons with previous methods. For all mpox skin lesion image detection baseline models, we finetuned there model in our proposed dataset, including the new open-source medical VLM Med-LLaVA.

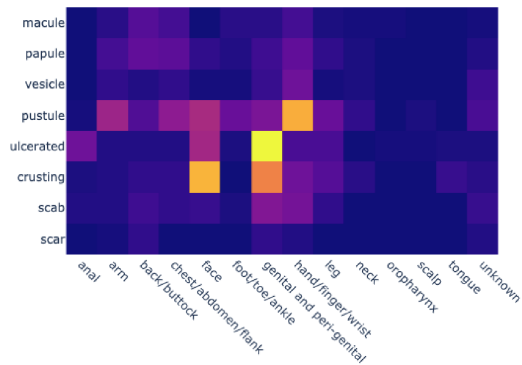


Figure 5: Heatmap illustrating the distribution of mpox across various body parts (x-axis) and stages of the disease (y-axis). The dataset covers nearly all body parts where mpox lesions are likely to occur. Although occurrences on areas such as the tongue and neck are very rare, these regions are still included in the dataset for completeness.

positive classifications made by the model. **Recall:** known as *sensitivity*, it assesses the proportion of actual positives correctly identified by the model, which is crucial in medicine for designing a screening test. **F1 Score:** the harmonic mean of precision and recall. It considers both false positives and false negatives. **AUROC:** The Area Under the Receiver Operating Characteristic curve represents the likelihood of the model distinguishing between classes. A higher AUROC score indicates better model performance.

### 4.3. Training Details.

As most prior papers did not provide open-sourced code, therefore, we reproduce their methods carefully and trained them on our dataset. We adopt a dataset split of **5:1:1 (2000:398:398)** for training, validation, and testing set, respectively. The split was done randomly based on patients' ID. The ratio of positive (mpox) and negative (non-mpox) is 4:7 in the test set.

The training setting for all baselines is the same. To preprocess the images, we also center-crop and resize the input images to  $336 \times 336$  resolution. The AdamW optimizer (Loshchilov and Hutter, 2017) with a weight decay set at 0.01 is also used to train all baselines and

MpoxVLM. Additionally, we employ a cosine annealing learning rate scheduler (Loshchilov and Hutter, 2016), with the base learning rate set at  $5 \times 10^{-5}$ . All baseline models are trained for 100 epochs and use early stops. The MpoxVLM is finetuned for 10,000 steps on 2 NVIDIA RTX 4090 GPUs using LoRA (Hu et al., 2021), with each GPU handling a batch size of 2. All codes and dataset details will be available upon acceptance.

#### 4.4. Compare with Previous Methods.

This section provides a comparative analysis of our method against existing approaches in the field. Previous studies (Bala et al., 2023; Thieme et al., 2023; Ahsan et al., 2022a; Jaradat et al., 2023; Altun et al., 2023) have predominantly employed CNN-based single network architectures. Our method demonstrates a significant improvement in performance over these CNN-based approaches. Conversely, another line of research, exemplified by Sitaula et al. (Sitaula and Shahi, 2022), utilizes an ensemble of multiple networks. Different from these methods, our method adopts the idea that LLM can enhance the performance of ViT in classification tasks (Chu et al., 2024) and uniquely leverages visual-language features extracted with general domain to enhance specific domain knowledge in the mpox diagnosis area.

#### 4.5. Compare with Multimodal LLMs.

As multimodal LLMs have been applied to various medical imaging tasks (Wu et al., 2023; Panagoulas et al., 2024) and are proved having basic understanding of mpox (Cheng et al., 2023), we also evaluated their ability to diagnose skin lesions caused by mpox virus infection. The input to these models included a system prompt: "Mpox is a zoonotic disease caused by the orthopoxvirus monkeypox virus. The example image is a patient with mpox. You are a helpful visual reasoning assistant that can distinguish mpox in new skin lesion images," along with an example mpox skin image. The experimental results, shown in Table 3, reveal that state-of-the-art multimodal LLMs, such as Claude 3 variants (Anthropic, 2024) and GPT-4o (Achiam et al., 2023), perform only marginally better than random guessing. Despite advancements, these models still struggle with fine-grained clinical tasks, suggesting that in their current unprimed state, they are not yet suitable for complex clinical applications. In contrast, the MpoxVLM framework achieves a significantly higher accuracy of 90.38%, underscoring

Multimodal LLMs	Accuracy(%) $\uparrow$
Claude 3 Haiku	53.07%
Claude 3 Sonnet	52.98%
Claude 3 Opus	52.48%
Claude 3.5 Sonnet	62.51%
GPT-4o-mini	67.22%
GPT-4o	76.45%
MpoxVLM (Ours)	<b>90.38%</b>

Table 3: Comparison with state-of-the-art Multimodal LLMs. Note: To let these closed source models answer the mpox skin lesion image questions, we use the same system prompt to provide LLMs related clinical background to mpox and use in-context learning to guide these models to answer the question.

Classifier	CLIP	Text	LLMs	Accuracy(%) $\uparrow$	AUROC(%) $\uparrow$
$\checkmark$	$\times$	$\times$	$\times$	87.94 $\pm$ 0.74	94.88 $\pm$ 0.88
$\times$	$\checkmark$	$\times$	$\checkmark$	87.34 $\pm$ 0.55	85.95 $\pm$ 0.73
$\times$	$\checkmark$	$\checkmark$	$\checkmark$	88.32 $\pm$ 0.12	88.44 $\pm$ 0.16
$\checkmark$	$\checkmark$	$\checkmark$	$\checkmark$	<b>90.38<math>\pm</math>0.80</b>	<b>95.16<math>\pm</math>0.72</b>

Table 4: Ablation study on different modules. The first row (Classifier only) refers to using only the Vision Transformer classifier for the task (similar to (Kularathne et al., 2024)). The second row (CLIP+LLMs) represents finetuning the LLaVA-based VLM baseline without incorporating additional Vision Transformer classifier module, with the model’s weights initialized by LLaVA-Med (Li et al., 2024). The third row (CLIP+Text+LLMs) refers to finetuning the VLM baseline while incorporating additional clinical history and demographic information about the patients. The fourth row showcases the results from MpoxVLM.

the importance of our new mpox skin image dataset in fine-tuning VLMs for precise mpox diagnosis.

#### 4.6. Ablation Study.

To validate the effectiveness of our model design, we conduct a detailed analysis of the individual contributions of various modules within our framework. We observe that even by freezing the weight of the CLIP model and only fine-tuning the LLM (LLaMA-2 7B), the performance can achieve relatively high accuracy similar to the previous SOTA method (line 2). Another key observation is the significant impact of the classification visual encoder on our framework’s performance. This is obvious in the marked improvement in the AUROC metric.

## 5. Discussion

Mpox exemplifies the domain gap issue expected in emerging diseases. Tools trained on initial, small datasets do not capture the diversity in a mature epidemic. Here an outbreak in a specific population spreads to a broader population requiring training of images of different lesion stages on a broad range of skin types and body parts. To ensure this, we use a significantly larger dataset than prior mpox computer vision approaches. This dataset encompasses a diverse demographic, mirroring those affected by mpox - as the epidemiology shifted from children in West and Central Africa to the Midwestern United States, to adults in Nigeria, and more broadly in MSM globally, with people of color disproportionately affected. The current mpox outbreak with new variant clade Ib has been affecting both adults and children in Burundi and the DRC, but with lower case positivity rates in children tested, we need to ensure accuracy in diagnosis, given the higher mortality rates of mpox in young children, but also the risks of isolating a young child and of not treating other causes of rash and illness. Images also reflect the range of mpox stages; many available images reflect the more easily identified, later images (such as the crusting umbilicated pustules in Fig 1) but fail to include earlier, less recognizable stages such as papules, whose identification would reduce transmission. Comparator diseases reflect both demographics and the global disease landscape against which mpox is identified. In addition, the images focus on the lesion alone, to avoid spurious correlations with clothing, backdrops, or even image quality, which may hint at disease geographies.

The scarcity of mpox images in the existing literature underscores the neglect of a disease known for 50 years to be endemic in West and Central Africa. In 2023, at least 581 people, mostly young children, likely died from mpox, with the case-fatality ratio attaining 8% in highly affected areas ([Organization, 2024](#)). However, many past dermatologic tools have included few images of persons of color or, as seen here, do not describe the demographics of the dataset. Such a tool will also need to be practical and achieve high accuracy, here 90%, and a high recall (sensitivity) for screening, and precision (positive predictive value) to assist in diagnosis where laboratory capacity is limited. Given the expected rise in novel and emerging diseases due to climate change and increased global movement, such an approach leads the way for further

tools to address novel diagnostic challenges ([Baker et al., 2022](#)).

## 6. Conclusion

Mpox has been historically neglected - first in Central and West Africa - and then in vulnerable populations globally including the LGBTQ community and disproportionately among people of color. The lack of attention to mpox has resulted in gaps in research and resources, particularly in dermatologic imaging and diagnosis. This paper outlined the first application of a vision-language model specifically tailored for dermatologic mpox images, alongside the largest fine-grained diagnostic dataset/benchmark for skin lesions caused by mpox. Our framework integrates clinical information such as mpox stages, affected body parts, gender, age, and Fitzpatrick skin types, making it the most comprehensive dataset for both AI researchers and clinicians. By developing this framework, we aim to provide a critical tool that supports clinicians in diagnosing mpox and, in the future, other emerging infectious diseases from skin lesion images. In future work, we aim to publish larger datasets containing more samples for each class and design the vision foundation model for digital dermatology.

## References

- Josh Achiam, Steven Adler, Sandhini Agarwal, Lama Ahmad, Ilge Akkaya, Florencia Leoni Aleman, Diogo Almeida, Janko Altenschmidt, Sam Altman, Shyamal Anadkat, et al. Gpt-4 technical report. *arXiv preprint arXiv:2303.08774*, 2023.
- Md Manjurul Ahsan, Muhammad Ramiz Uddin, Mithila Farjana, Ahmed Nazmus Sakib, Khondhaker Al Momin, and Shahana Akter Luna. Image data collection and implementation of deep learning-based model in detecting monkeypox disease using modified vgg16. *arXiv preprint arXiv:2206.01862*, 2022a.
- Md Manjurul Ahsan, Muhammad Ramiz Uddin, and Shahana Akter Luna. Monkeypox image data collection. *arXiv preprint arXiv:2206.01774*, 2022b.
- Jean-Baptiste Alayrac, Jeff Donahue, Pauline Luc, Antoine Miech, Iain Barr, Yana Hasson, Karel Lenc, Arthur Mensch, Katherine Millican, Malcolm Reynolds, et al. Flamingo: a visual language model for few-shot learning. *NeurIPS*, 2022.

- Shams Nafisa Ali, Md Tazuddin Ahmed, Tasnim Jahan, Joydip Paul, SM Sani, Nawsabah Noor, Anzirun Nahar Asma, and Taufiq Hasan. A web-based mpox skin lesion detection system using state-of-the-art deep learning models considering racial diversity. *arXiv preprint arXiv:2306.14169*, 2023.
- Lao-Tzu Allan-Blitz and Jeffrey D Klausner. Prevalence of mpox immunity among the core group and its potential to prevent future large-scale outbreaks. *The Lancet Microbe*, 2024.
- Murat Altun, Hüseyin Gürüler, Osman Özkaraca, Faheem Khan, Jawad Khan, and Youngmoon Lee. Monkeypox detection using cnn with transfer learning. *Sensors*, 2023.
- Anthropic. Claude 3 family. <https://www.anthropic.com/news/claude-3-family>, 2024. Accessed: 2024-05-27.
- Rachel Baker, Ayesha Mahmud, Ian Miller, Malavika Rajeev, Ridisoa Rasambainarivo, Benjamin Rice, et al. Infectious disease in an era of global change. *Nature Review Microbiology*, 2022.
- Diponkor Bala, Md Shamim Hossain, Mohammad Alamgir Hossain, Md Ibrahim Abdullah, Md Mizanur Rahman, Balachandran Manavalan, Naijie Gu, Mohammad S Islam, and Zhangjin Huang. Monkeynet: A robust deep convolutional neural network for monkeypox disease detection and classification. *Neural Networks*, 2023.
- Catarina Barata, Jorge S Marques, and M Emre Celebi. Deep attention model for the hierarchical diagnosis of skin lesions. In *CVPRW*, 2019.
- Amanda Bleichrodt, Ruiyan Luo, Alexander Kirpich, and Gerardo Chowell. Evaluating the forecasting performance of ensemble sub-epidemic frameworks and other time series models for the 2022–2023 mpox epidemic. *Royal Society Open Science*, 11(7): 240248, 2024.
- Nicola Bragazzi, Woldegebriel Woldegerima, Sarafa Iyaniwura, Qing Han, Xiaoying Wang, Aminath Shausan, Kingsley Badu, Patrick Okwen, Cheryl Prescod, Michelle Westin, Andrew Omame, Manlio Converti, Bruce Mellado, Jianhong Wu, and Jude Kong. Knowing the unknown: The underestimation of monkeypox cases. insights and implications from an integrative review of the literature. *Frontiers in Microbiology*, 2022.
- Joel G Breman, MV Steniowski, E Zanotto, AI Gromyko, I Arita, et al. Human monkeypox, 1970-79. *Bulletin of the World Health Organization*, 58(2):165, 1980.
- Krishnaraj Chadaga, Srikanth Prabhu, Niranjana Sampathila, Sumith Nireswalya, Swathi S Katta, Ru-San Tan, and U Rajendra Acharya. Application of artificial intelligence techniques for monkeypox: a systematic review. *Diagnostics*, 13(5):824, 2023.
- Zhe Chen, Jiannan Wu, Wenhai Wang, Weijie Su, Guo Chen, Sen Xing, Muyan Zhong, Qinglong Zhang, Xizhou Zhu, Lewei Lu, et al. Internvl: Scaling up vision foundation models and aligning for generic visual-linguistic tasks. In *CVPR*, 2024.
- Kunming Cheng, Yongbin He, Cheng Li, Ruijie Xie, Yanqiu Lu, Shuqin Gu, and Haiyang Wu. Talk with chatgpt about the outbreak of mpox in 2022: reflections and suggestions from ai dimensions. *Annals of Biomedical Engineering*, 2023.
- Xiangxiang Chu, Jianlin Su, Bo Zhang, and Chunhua Shen. Visionllama: A unified llama interface for vision tasks. *arXiv preprint arXiv:2403.00522*, 2024.
- Fabian Gröger, Simone Lionetti, Philippe Gottfrois, Alvaro Gonzalez-Jimenez, Matthew Groh, Roxana Daneshjou, Alexander A Navarini, Marc Pouly, Labelling Consortium, et al. Towards reliable dermatology evaluation benchmarks. In *Machine Learning for Health (ML4H)*, 2023.
- Jeannette Guarner, Carlos Del Rio, and Preeti N Malani. Monkeypox in 2022—what clinicians need to know. *Jama*, 328(2):139–140, 2022.
- Emily Harris. Who: as mpox outbreaks continue, cases may be underestimated. *JAMA*, 331(24):2070–2070, 2024.
- Kaiming He, Xinlei Chen, Saining Xie, Yanghao Li, Piotr Dollár, and Ross Girshick. Masked autoencoders are scalable vision learners. In *CVPR*, 2022.
- Edward J Hu, Yelong Shen, Phillip Wallis, Zeyuan Allen-Zhu, Yuanzhi Li, Shean Wang, Lu Wang, and Weizhu Chen. Lora: Low-rank adaptation of large language models. *arXiv preprint arXiv:2106.09685*, 2021.
- Joana Palés Huix, Adithya Raju Ganeshan, Johan Fredin Haslum, Magnus Söderberg, Christos Matsoukas, and Kevin Smith. Are natural domain

- foundation models useful for medical image classification? In *WACV*, 2024.
- Towhidul Islam, Mohammad Arafat Hussain, Forhad Uddin Hasan Chowdhury, and BM Riazul Islam. A web-scraped skin image database of monkeypox, chickenpox, smallpox, cowpox, and measles. *bioRxiv*, pages 2022–08, 2022.
- Ameera S Jaradat, Rabia Emhamed Al Mamlook, Naif Almakayeel, Nawaf Alharbe, Ali Saeed Almuflih, Ahmad Nasayreh, Hasan Gharaibeh, Mohammad Gharaibeh, Ali Gharaibeh, and Hanin Bzizi. Automated monkeypox skin lesion detection using deep learning and transfer learning techniques. *International Journal of Environmental Research and Public Health*, 2023.
- Menglin Jia, Luming Tang, Bor-Chun Chen, Claire Cardie, Serge Belongie, Bharath Hariharan, and Ser-Nam Lim. Visual prompt tuning. In *ECCV*, 2022.
- Saddam Hussain Khan, Rashid Iqbal, and Saeeda Naz. A recent survey of the advancements in deep learning techniques for monkeypox disease detection. *arXiv preprint arXiv:2311.10754*, 2023.
- Yudara Kularathne, Prathapa Janitha, Sithira Ambepitiya, Prarthathanan Sothyrajah, Thanveer Ahamed, and Dinuka Wijesundara. Mpox detection advanced: Rapid epidemic response through synthetic data. *arXiv preprint arXiv:2407.17762*, 2024.
- Henry Laurensen-Schafer, Nikola Sklenovská, Ana Hoxha, Steven M Kerr, Patricia Ndumbi, Julia Fitzner, Maria Almiron, Luis Alves de Sousa, Sylvie Briand, Orlando Cenciarelli, et al. Description of the first global outbreak of mpox: an analysis of global surveillance data. *The Lancet Global Health*, 11(7):e1012–e1023, 2023.
- Chunyuan Li, Cliff Wong, Sheng Zhang, Naoto Usuyama, Haotian Liu, Jianwei Yang, Tristan Naumann, Hoifung Poon, and Jianfeng Gao. Llava-med: Training a large language-and-vision assistant for biomedicine in one day. *NeurIPS*, 2024.
- Junnan Li, Dongxu Li, Silvio Savarese, and Steven Hoi. Blip-2: Bootstrapping language-image pre-training with frozen image encoders and large language models. *arXiv preprint arXiv:2301.12597*, 2023a.
- Yunxiang Li, Zihan Li, Kai Zhang, Ruilong Dan, Steve Jiang, and You Zhang. Chatdoctor: A medical chat model fine-tuned on a large language model meta-ai (llama) using medical domain knowledge. *Cureus*, 2023b.
- Haotian Liu, Chunyuan Li, Yuheng Li, and Yong Jae Lee. Improved baselines with visual instruction tuning. *arXiv preprint arXiv:2310.03744*, 2023.
- Haotian Liu, Chunyuan Li, Qingyang Wu, and Yong Jae Lee. Visual instruction tuning. *NeurIPS*, 2024.
- Yuan Liu, Ayush Jain, Clara Eng, David H Way, Kang Lee, Peggy Bui, Kimberly Kanada, Guilherme de Oliveira Marinho, Jessica Gallegos, Sara Gabriele, et al. A deep learning system for differential diagnosis of skin diseases. *Nature medicine*, 2020.
- Ilya Loshchilov and Frank Hutter. Sgdr: Stochastic gradient descent with warm restarts. *arXiv preprint arXiv:1608.03983*, 2016.
- Ilya Loshchilov and Frank Hutter. Decoupled weight decay regularization. *arXiv preprint arXiv:1711.05101*, 2017.
- Junjie Lu, Hui Xing, Chunhua Wang, Mengjun Tang, Changcheng Wu, Fan Ye, Lijuan Yin, Yang Yang, Wenjie Tan, and Liang Shen. Mpox (formerly monkeypox): pathogenesis, prevention, and treatment. *Signal Transduction and Targeted Therapy*, 8(1): 458, 2023.
- Nicolas Luna, Angie L Ramírez, Marina Muñoz, Nathalia Ballesteros, Luz H Patiño, Sergio Andres Castañeda, D Katterine Bonilla-Aldana, Alberto Paniz-Mondolfi, and Juan David Ramírez. Phylogenomic analysis of the monkeypox virus (mpxv) 2022 outbreak: Emergence of a novel viral lineage? *Travel medicine and infectious disease*, 49:102402, 2022.
- Kristen E Marshall, Marlee Barton, Janell Nichols, et al. Health care personnel exposures to subsequently laboratory-confirmed monkeypox patients—colorado, 2022. *American Journal of Transplantation*, 2022.
- Oriol Mitjà, Andrea Alemany, Michael Marks, Jezer I Lezama Mora, Juan Carlos Rodríguez-Aldama, Mayara Secco Torres Silva, Ever Arturo Corral Herrera, Brenda Crabtree-Ramirez, José Luis Blanco,

- Nicolo Girometti, et al. Mpox in people with advanced hiv infection: a global case series. *The Lancet*, 401(10380):939–949, 2023a.
- Oriol Mitjà, Dimie Ogoina, Boghuma K Titanji, Cristina Galvan, Jean-Jacques Muyembe, Michael Marks, and Chloe M Orkin. Monkeypox. *The Lancet*, 2023b.
- Jesutofunmi A Omiye, Haiwen Gui, Shawheen J Rezaei, James Zou, and Roxana Daneshjou. Large language models in medicine: The potentials and pitfalls: A narrative review. *Annals of Internal Medicine*, 2024.
- World Health Organization. Who’s operational update on health emergencies. *World Health Organization Situation Report March 2024*, 2024.
- Dimitrios P Panagoulas, Maria Virvou, and George A Tsihrintzis. Evaluating llm-generated multimodal diagnosis from medical images and symptom analysis. *arXiv preprint arXiv:2402.01730*, 2024.
- Jonathan E Pekar, Yu Wang, Jade C Wang, Yucai Shao, Faten Taki, Lisa A Forgione, Helly Amin, Tyler Cabby, Kimberly Johnson, Lucia V Torian, et al. Genomic epidemiology reveals 2022 mpox epidemic in new york city governed by heavy-tailed sexual contact networks. *medRxiv*, pages 2024–07, 2024.
- Alec Radford, Jong Wook Kim, Chris Hallacy, Aditya Ramesh, Gabriel Goh, Sandhini Agarwal, Girish Sastry, Amanda Askell, Pamela Mishkin, Jack Clark, et al. Learning transferable visual models from natural language supervision. In *ICML*, 2021.
- Shailima Rampogu. A review on the use of machine learning techniques in monkeypox disease prediction. *Science in One Health*, page 100040, 2023.
- Caitlin Rivers, Crystal Watson, and Alexandra L Phelan. The resurgence of mpox in africa. *JAMA*, 332(13):1045–1046, 2024.
- Nataniel Ruiz, Yuanzhen Li, Varun Jampani, Yael Pritch, Michael Rubinstein, and Kfir Aberman. Dreambooth: Fine tuning text-to-image diffusion models for subject-driven generation. In *CVPR*, 2023.
- Veysel Harun Sahin, Ismail Oztel, and Gozde Yolcu Oztel. Human monkeypox classification from skin lesion images with deep pre-trained network using mobile application. *Journal of Medical Systems*, 46(11):79, 2022.
- Emily A Siegrist and Joseph Sassine. Antivirals with activity against mpox: a clinically oriented review. *Clinical infectious diseases*, 76(1):155–164, 2023.
- Chiranjibi Sitaula and Tej Bahadur Shahi. Monkeypox virus detection using pre-trained deep learning-based approaches. *Journal of Medical Systems*, 2022.
- Elena Sizikova, Joshua Vendrow, Xu Cao, Rachel Grotheer, Jamie Haddock, Lara Kassab, Alona Kryshchenko, Thomas Merkh, RWMA Madushani, Kenny Moise, et al. Automatic infectious disease classification analysis with concept discovery. *arXiv preprint arXiv:2209.02415*, 2022.
- Nyi Nyi Soe, Zhen Yu, Phyu Mon Latt, David Lee, Ranjit Singh Samra, Zongyuan Ge, Rashidur Rahman, Jiajun Sun, Jason J Ong, Christopher K Fairley, et al. Using ai to differentiate mpox from common skin lesions in a sexual health clinic: algorithm development and validation study. *Journal of Medical Internet Research*, 26:e52490, 2024.
- Gemini Team, Rohan Anil, Sebastian Borgeaud, Yonghui Wu, Jean-Baptiste Alayrac, Jiahui Yu, Radu Soricut, Johan Schalkwyk, Andrew M Dai, Anja Hauth, et al. Gemini: a family of highly capable multimodal models. *arXiv preprint arXiv:2312.11805*, 2023.
- Alexander H Thieme, Yuanning Zheng, Gautam Machiraju, Chris Sadee, Mirja Mittermaier, Maximilian Gertler, Jorge L Salinas, Krithika Srinivasan, Prashna Gyawali, Francisco Carrillo-Perez, et al. A deep-learning algorithm to classify skin lesions from mpox virus infection. *Nature medicine*, 2023.
- Hugo Touvron, Louis Martin, Kevin Stone, Peter Albert, Amjad Almahairi, Yasmine Babaei, Nikolay Bashlykov, Soumya Batra, Prajjwal Bhargava, Shruti Bhosale, et al. Llama 2: Open foundation and fine-tuned chat models. *arXiv preprint arXiv:2307.09288*, 2023.
- Chaoyi Wu, Jiayu Lei, Qiaoyu Zheng, Weike Zhao, Weixiong Lin, Xiaoman Zhang, Xiao Zhou, Ziheng Zhao, Ya Zhang, Yanfeng Wang, et al. Can gpt-4v (ision) serve medical applications? case studies on gpt-4v for multimodal medical diagnosis. *arXiv preprint arXiv:2310.09909*, 2023.

Renrui Zhang, Jiaming Han, Aojun Zhou, Xiangfei Hu, Shilin Yan, Pan Lu, Hongsheng Li, Peng Gao, and Yu Qiao. Llama-adapter: Efficient fine-tuning of language models with zero-init attention. *arXiv preprint arXiv:2303.16199*, 2023.

Juexiao Zhou and Xin Gao. Skingpt: A dermatology diagnostic system with vision large language model. *arXiv preprint arXiv:2304.10691*, 2023.

Deyao Zhu, Jun Chen, Xiaoqian Shen, Xiang Li, and Mohamed Elhoseiny. Minigt-4: Enhancing vision-language understanding with advanced large language models. *arXiv preprint arXiv:2304.10592*, 2023.

Mohammad Ali Zinnah, Md Bashir Uddin, Tanjila Hasan, Shobhan Das, Fahima Khatun, Md Hasibul Hasan, Ruenruetai Udonsom, Md Masudur Rahman, and Hossam M Ashour. The re-emergence of mpox: old illness, modern challenges. *Biomedicines*, 12(7):1457, 2024.

Table 5: Skin Color Fitzpatrick Scale

Number	Description
0	Unknown
1	Always burns, never tans (palest; freckles)
2	Usually burns, tans minimally (light colored but darker than fair)
3	Sometimes mild burn, tans uniformly (golden honey or olive)
4	Burns minimally, always tans well (moderate brown)
5	Very rarely burns, tans very easily (dark brown)
6	Never burns (deeply pigmented dark brown to darkest brown)

## Appendix A. Description of Dataset Terms

This appendix provides a detailed explanation of the terms used in our dataset, explaining the meaning of the numbers corresponding to different attributes. Table 5 describes the Fitzpatrick Skin Type Scale, which categorizes skin types based on their response to sun exposure. The numerical values in this table range from 0 (Unknown) to 6, with each number representing a specific skin type. The scale is widely used in dermatology to classify different levels of melanin in the skin, influencing susceptibility to sunburn and skin cancer risk.

Table 6 provides the body parts where mpox lesions can be observed. Each body part is assigned a numerical value from 0 (Unknown) to 11, with each number corresponding to a specific region of the body.

Table 7 lists the different diseases or conditions in the dataset and assigns each a corresponding numerical value. The numbers range from 0 (Unknown disease) to 86, covering a wide range of skin-related infections, inflammatory conditions, and benign or malignant skin lesions. This table is important for annotating and diagnosing different dermatologic conditions alongside mpox.

Table 6: Body Part

Number	Body Part
0	Unknown
1	Hand/finger/wrist
2	Foot/toe/ankle
3	Arm
4	Leg
5	Chest/Abdomen/flank
6	Back/Buttock
7	Face
8	Neck
9	Genital and peri-genital
10	Anal
11	Scalp

Table 7: Disease in the data.

Number	Disease	Number	Disease
0	Unknown	43	Other folliculitis
1	Varicella (chickenpox)	44	Other mycobacterial infections
2	Herpes zoster (shingles)	45	Bartonella
3	Measles	46	PLEVA
4	Herpes - extra-genital	47	Other rickettsia or scrub typhus
5	Herpes - genital	48	Melioidosis
6	Syphilis primary or congenital	49	Lichen Planus
7	Syphilis secondary	50	Buruli Ulcer
8	Erythema Migrans	51	Talaromyces marneffeii
9	Healed Scar	52	Coccidioidomycosis
10	Acne	53	Paracoccidioidomycosis
11	Molluscum	54	Sporotrichosis
12	Scabies	55	Fusarium
13	Hives, urticaria	56	Leukemic Cutis
14	Skin cancer	57	Eczema
15	Tularemia	58	Roseola
16	Blastomycosis	59	Perforating Dermatoses
17	Hand foot and mouth disease	60	Disseminated Gonorrhoea
18	Impetigo or ecthyma	61	Dermatitis herpetiformis
19	Bed bug bites	62	Prurigo Nodularis
20	Other insect bites	63	Nipple disorder
21	Genital warts (HPV)	64	Drug Eruption
22	Furunculosis or early abscesses	65	Bullous Pemphigoid
23	Folliculitis (standard bacterial)	66	Dermatofibroma
24	Miliaria	67	Plain skin (no disease)
25	Tuberculosis	68	Nipple (no disease)
26	BCG vaccination	69	Genital skin (no disease)
27	Lymphangioma circumscriptum	70	Anal area (no disease)
28	Spider bite	71	Oral lips (no disease)
29	Herpes gestationis	72	Nose (no disease)
30	Donovanosis	73	Scalp with hair (no disease)
31	Behcet's	74	Beard (no disease)
32	Leishmaniasis	75	Hemorrhoid
33	Chancroid	76	Anal (no disease)
34	Erythema multiforme	77	Freckled skin (no disease)
35	Toxoplasmosis	78	Mole (no disease)
36	Histoplasmosis	79	Pyogenic granuloma
37	Rickettsia Akari	80	Janeway lesions
38	Cryptococcus	81	Palm (no disease)
39	Degos	82	Buttock (no disease)
40	Rickettsia parkeri	83	Teeth (no disease)
41	Pityriasis rosea	84	Teeth (caries)
42	Psoriasis (guttate)	85	Anthrax
		86	Malakoplakia